SUBBAND OPTIMIZATION AND FILTERING TECHNIQUE FOR PRACTICAL PERSONAL AUDIO SYSTEMS

Hyungjun So and Jung-Woo Choi

School of Electrical Engineering,
Korea Advanced Institute of Science and Technology (KAIST)

ABSTRACT

The implementation of personal audio systems in enclosed spaces, such as a car cabin, suffers from severe echoes from surrounding boundaries. In order to focus sound energy on a single seat position, echoes should be controlled by long multichannel filters with up to a few thousand taps for each channel, which leads to increased memory size and computational complexity. In an attempt to design a practical personal audio system, a subband based optimization and filtering technique are proposed. The design of optimal filters for downsampled low frequency responses enables finer control of low frequency echoes without significantly increasing the number of filter taps, while the broadband response of high frequency components can be controlled with a fewer number of filter taps. Experiments conducted in a real car cabin demonstrate that more than 20 dB SPL difference can be achieved across different seat positions with only half the number of filter taps.

Index Terms— Personal audio, Subband optimization

1. INTRODUCTION

Personal audio systems [1-5, 11, 21] aim to produce an isolated sound zone using interferences of sound waves from multiple loudspeakers. Sound waves are controlled to form constructive interferences inside a selected zone, while sounds propagating to other areas are suppressed. In order to manipulate the interference pattern, the impulse responses (IRs) of multiple loudspeakers are measured, and this information is used to design multichannel filters that control the sound radiation from individual loudspeakers.

A basic schematic of the personal audio system is shown in Figure 1. A single input signal X, which is the sound we want to deliver to the selected zone, is fed into the multichannel personal audio filter (MPAF) $Q^{(n)}$ consisting of N channel FIR filters. The filtered signal $Y^{(n)}$ drives the n^{th} loudspeaker (n=1, $\cdots$, N), and the sounds emitted from all loudspeakers propagate in space. In the frequency domain, the sound propagation can be represented in terms of the frequency responses $G^{(m,n)}$ between the m^{th} microphone and the n^{th} loudspeaker, which leads to the following expression for the pressure field $P^{(m)}$ at the microphone's position:

$$P^{(m)}(e^{j\omega}) = X(e^{j\omega})\sum_{n=1}^{N} G^{(m,n)}(e^{j\omega})Q^{(n)}(e^{j\omega}) \quad (1)$$

Using matrix notations $[\mathbf{G}]_{(m,n)} = G^{(m,n)}$, $[\mathbf{p}]_{(m,1)} = P^{(m)}$ and $[\mathbf{q}]_{(n,1)} = Q^{(n)}$, (1) can be rewritten as $\mathbf{p} = X(e^{j\omega})\mathbf{G}\mathbf{q}$. The objective of personal audio is to find the optimal MPAF coefficients $\mathbf{q}$ using the measured information $\mathbf{G}$.

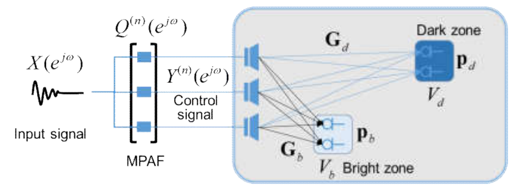

Figure 1. Schematic of the personal audio system

For the design of MPAF, various optimization strategies have been proposed. In [6-10], an acoustically bright zone (V_b) and a dark zone (V_d) (Figure 1) were defined, and the potential energy ratio between the two zones was maximized such that the zones of loud and quiet sound can be generated at the same time. Denoting the frequency response matrices corresponding to the bright and dark zones as $\mathbf{G}_b$ and $\mathbf{G}_d$, respectively, the energy ratio between the two zones can be written as:

$$\beta = (\mathbf{q}^H\mathbf{G}_b^H\mathbf{G}_b\mathbf{q}) / (\mathbf{q}^H\mathbf{G}_d^H\mathbf{G}_d\mathbf{q}) . \quad (2)$$

This energy ratio, denoted as the acoustic contrast (AC), only concerns the acoustic potential energy over selected zones, and hence, neglects the magnitude and phase variations in space.

Another popular approach, the pressure matching (PM) technique [12-15], defines a target sound field over the zone of interest and tries to minimize the error between the target and reproduced sound fields. The introduction of the target sound field can reduce the pressure field variation within the selected zones, but it is hard to guarantee that the pre-defined target sound field is the best for the realization of a personal audio. In addition, lots of control effort can be wasted by mimicking the shape of the sound field rather than for the sound isolation. For this reason, many hybrid approaches [11, 16-20] take advantage of both techniques.

One of the major problems in realizing a personal audio system is the complex acoustic propagation characteristics in an enclosed space. For example, in a small acoustic space such as a car cabin (e.g., Figure 2(b)), the sound propagation contains a lot of early reflections, as well as late reverberations (Figure 3(a)). The first study on the personal audio in a car cabin was reported by Cheer *et al.* [5]. In this study, the sound field was controlled by four woofers added on doors and eight directional loudspeakers attached near the headrests. Although only two microphones for each seat were used for the control and evaluation, it was demonstrated that a certain amount of SPL difference can be produced. Several attempts have followed [9, 21] by directly maximizing the acoustic contrast or pressure matching using active

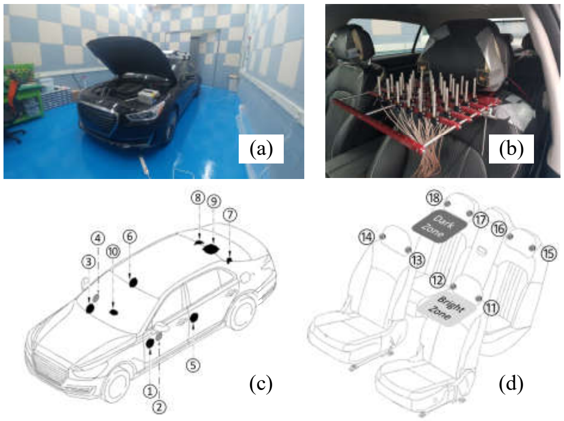

Figure 2. Experiment configuration: (a) test vehicle, (b) microphone array (c) positions of factory-installed loudspeakers (d) positions of headrest loudspeakers.

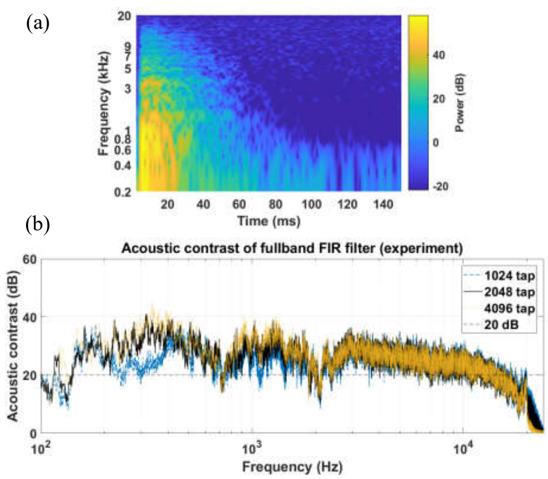

Figure 3. (a) Spectrogram of the measured IR of a center loudspeaker (No. 10 of Figure 2(c)). (b) Achieved acoustic contrasts with respect to the number of filter taps.

noise cancellation. For example, Choi [9] has shown that acoustic contrast over 20 dB can be achieved under 1 kHz for a standard vehicle with factory installed loudspeakers.

In a car cabin, the FIR filtering of MPAFs requires a lot of computational effort. As for example, the acoustic contrasts for different taps of FIR filters are measured using the 18 channels loudspeaker setup described in Figure 2 and Section 3. The results obtained from the acoustic contrast maximization (Figure 3(b)) show that long filters of more than 2048 taps are required to achieve high acoustic contrast. This is because the low frequency response has very long reverberations lasting over 100 ms (Figure 3(a)). On the other hand, the gain in acoustic contrast from increasing further the filter length (4096 tap) is not significant.

Real-time filtering of 18 channel FIR filters of 2048 taps is impractical, because of the required memory size and computational cost. In this work, we propose a more efficient technique based on the subband filtering structure.

2. SUBBAND FILTERING

2.1 Quadrature mirror filtering structure

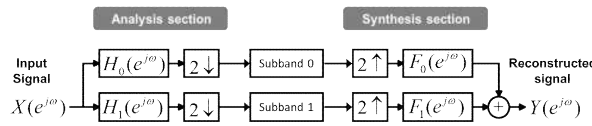

Figure 4. Basic single stage quadrature mirror filter (QMF) structure

Among many possible choices of subband filtering structures, quadrature mirror filters (QMFs) [22-30] can provide temporarily localized, orthogonal multiscale transform. It suppresses the aliasing accompanied by the analysis/synthesis filter structure in terms of the constraint imposed on possible filter shapes. Consider a two-band problem dividing the system into low and high subband of equal size (Figure 4). The output $Y(z)$ from the input $X(z)$ filtered by the low and high-pass analysis filters $H_0(z)$, $H_1(z)$ and synthesis filters $F_0(z)$, $F_1(z)$ can be written as:

$$\begin{aligned} Y(z) &= \tfrac{1}{2}\left[H_0(z)F_0(z)+H_1(z)F_1(z)\right]X(z) \\ &\quad + \tfrac{1}{2}\left[H_0(-z)F_0(z)+H_1(-z)F_1(z)\right]X(-z), \end{aligned} \tag{3}$$

where the first bracketed term is the system's response, and the second term denotes the aliasing. As is well known, the paraunitary QMF filter [25] of length S constrained by the equation:

$$\begin{aligned} &H_1(z) = -z^{-(S-1)}H_0(-z^{-1}) \\ &F_0(z) = z^{-(S-1)}H_0(z^{-1}),\ F_1(z) = z^{-(S-1)}H_1(z^{-1}), \end{aligned} \tag{4}$$

can yield the perfect cancellation of the aliasing, as well as the simplified response on the unit circle:

$$Y(e^{j\omega}) = \tfrac{1}{2}e^{-j(S-\omega)}[|H_0(e^{j\omega})|^2 + |H_0(e^{j(\pi-\omega)})|^2]X(e^{j\omega})\,. \tag{5}$$

If the subband filter satisfies the following power complementary property

$$\left|H_0(e^{j\omega})\right|^2 + \left|H_0(e^{j(\pi-\omega)})\right|^2 = 2\,, \tag{6}$$

then one can reconstruct the delayed original input signal $X(e^{j\omega})e^{-j(S-1)\omega}$ without any distortion. However, a perfect reconstruction filter has poor frequency selectivity, so various techniques to find the best trade-off between the amount of distortion and the frequency selectivity have been proposed [23-26]. The multiband processing can also be realized through the multi-level pyramid cascade of the two-band analysis/synthesis system.

In the personal audio system, a single input signal representing music or speech to be reproduced is filtered by the analysis filters and then downsampled. Each downsampled subband signal is then fed into the MPAFs optimized based on the frequency responses for that subband (Figure 5). The results are the multichannel outputs, each of which passes through the upsampler and the synthesis filter. The subband outputs of the same channel are then combined to construct the final playback signal $Y^{(n)}$ for the n^{th} loudspeaker.

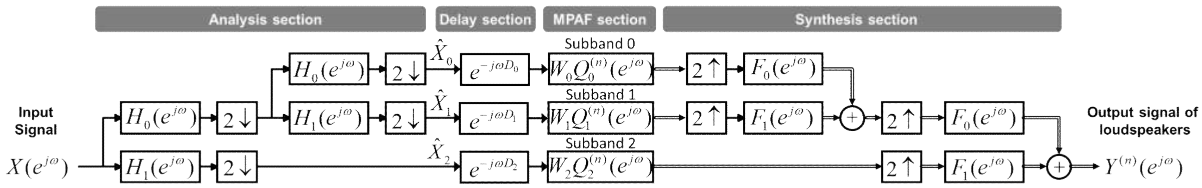

Figure 5. Subband filtering structure for multichannel personal audio filters (⟶ : single channel signal, ⟹ : multichannel signals)

2.2 Subband optimization for personal audio

For the subband filtering structure, the MPAF coefficients of the i^{th} subband $Q_i^{(n)}$ should be optimized for that subband. Since the required filter length varies depending on the frequency region, the multichannel filter optimized for each subband can have a reduced length.

The procedure to optimize MPAF for each subband is a bit different from the conventional technique. Although both the frequency domain [6-9] or time domain [10, 11] designs can be incorporated, here we have adopted the frequency domain approach for simplicity. First, each of the IRs $G^{(m,n)}(k)$ between the n^{th} loudspeaker and m^{th} microphone with the temporal index k is passed through the subband analysis filter to obtain the downsampled IR $G_i^{(m,n)}(k)$ of the i^{th} subband. Then the IRs are zero padded and Fourier transformed to obtain the frequency responses $G_i^{(m,n)}(e^{j\omega})$. For each frequency bin of the subband, the cost function involved with the acoustic contrast and input power can be defined as follows [8]:

$$\gamma_i = \frac{\mathbf{q}_i^H \mathbf{G}_{b,i}^H \mathbf{G}_{b,i} \mathbf{q}_i}{\mathbf{q}_i^H \mathbf{G}_{d,i}^H \mathbf{G}_{d,i} \mathbf{q}_i + \lambda_i \mathbf{q}_i^H \mathbf{q}_i}, \tag{7}$$

where $\mathbf{G}_{b,i}$, $\mathbf{G}_{d,i}$ are matrices whose $(m,n)^{\text{th}}$ element are given by $G_{b,i}^{(m,n)}$, $G_{d,i}^{(m,n)}$, respectively, and $\mathbf{q}_i = [Q_i^{(1)}(e^{j\omega}), \cdots, Q_i^{(N)}(e^{j\omega})]^T$ is the vector of the prototype MPAF coefficients. The tuning parameter λ_i penalizes the cost function in proportion to the input power $\mathbf{q}_i^H \mathbf{q}_i$, which is introduced to ensure the power efficiency of the optimal solution. The optimal solution, i.e., the direction of the MPAF vector $\mathbf{q}_i$ maximizing γ_i can be found through the eigenvalue analysis, which yields optimal $\mathbf{q}_i(e^{j\omega_k})$ of unit magnitude for discrete frequencies ω_k ($k = 1, \cdots, K_i$). At this stage, the absolute magnitude and common phase of $\mathbf{q}_i$ are undetermined, but they can be derived by introducing additional constraint to minimize the distortion of the pressure response at a reference position.

The simple way described in [7] is to define a target response at a reference position (microphone m_{ref}) and minimize the reproduction error. For a frequency response vector defined at the reference position $\mathbf{g}_i(e^{j\omega_k}) = [G_i^{(m_{ref},1)}(e^{j\omega_k}), \cdots, G_i^{(m_{ref},N)}(e^{j\omega_k})]^T$, the pressure at the reference position is given by

$$P_i(e^{j\omega_k}) = W_i(e^{j\omega_k}) \mathbf{g}_i^T(e^{j\omega_k}) \mathbf{q}_i(e^{j\omega_k}), \tag{8}$$

where the weight $W_i(e^{j\omega_k})$ can be regarded as an equalization filter that matches the magnitude and phase of MPAFs to those of a target response P_i. For this subband approach, the target response can be defined as the delayed impulse response of the analysis filter section. That is, the output $\hat{X}_i(e^{j\omega_k})$ of the analysis filter section (Figure 5) for the input signal given by the unit impulse $X(e^{j\omega_k}) = 1$ is set as the target response P_i. Since the filter coefficients designed at discrete frequencies induce cyclic repetition in the time domain, the target response for each subband can include a modeling delay $P_i(e^{j\omega_k}) = \hat{X}_i(e^{j\omega_k}) e^{-j\omega_k D_M}$ to align the filter coefficients in the time domain. By matching the expected sound output of each subband to the delayed impulse response of the analysis filter, the final response after the synthesis filter can be reconstructed with minimal distortion. From (8), the weight $W_i(e^{j\omega_k})$ minimizing the reproduction error is given by

$$W_i(e^{j\omega_k}) = \left(\mathbf{g}_i^T(e^{j\omega_k}) \mathbf{q}_i(e^{j\omega_k}) + \eta_i(e^{j\omega_k})\right)^{-1} P_i(e^{j\omega_k}). \tag{9}$$

Note that the additional regularization using the constant η_i is also incorporated at this stage, to prevent the excessive amplification of W_i during the equalization.

The equalized subband MPAF filters $W_i \mathbf{q}_i$ are then transformed to time domain signals $Q_i^{(n)}(\ell)$ using the inverse Fourier transform and then truncated to finite lengths (L_i). To compensate for the different starting positions of the truncated filters and to adjust the non-identical filtering delay of multistage analysis/synthesis filter, additional delay lines with integer delay D_i are added before the MPAF section (Figure 5). The choice of filter length L_i does influence the performance of a personal audio system, so the smallest number of taps that does not significantly reduce the acoustic contrast is selected by inspecting the acoustic contrast variation for different numbers of filter taps.

3. APPLICATION TO THE TEST VEHICLE

To verify the proposed technique, the IRs measured in a car cabin were optimized for each subband. The test vehicle selected was the Hyundai Genesis G90 with 10 independent loudspeakers installed on four door panels, center fascia, and a rear shelf (Figure 2(c)). For the high-frequency control, two additional loudspeakers were installed at each headrest (Figure 2(d)), thereby a total of 18 loudspeakers were used. The IRs were measured by 30 microphones (G.R.A.S type 40ph) arranged in a 6×5 rectangular array with 5 cm intervals.

The measured IRs are 9600 taps long at f_s = 48 kHz, and these IRs were processed by five analysis stages (10 high and low-pass filters in total) for the following cutoff frequencies: 0.75, 1.5, 3, 6, and 12 kHz. Each subband filter was designed from the equiripple prototype filter of 25 taps, using the Matlab script firpr2chfb.m. The lengths of the downsampled IRs are: 300, 300, 600, 1200, 2400, and 4800 taps.

MPAFs of different L_i were designed for six subband IRs extracted from five subband filters. The acoustically bright and dark zones were set at the driver's seat and rear-right passenger seat positions, respectively. The regularization parameter λ_i of (7) was determined such that the ratio of bright zone energy to the input power $(\mathbf{q}_i^H \mathbf{G}_{b,i}^H \mathbf{G}_{b,i} \mathbf{q}_i) / \mathbf{q}_i^H \mathbf{q}_i$ is no less than 6 dB from the maximum. Another regularization filter η_i for the equalization was set to 0.1% of the RMS averaged pressure of the bright zone. By inspecting the acoustic contrast with respect to different number of filter taps, the lengths of FIR filters for individual subbands were determined as shown in Table 1.

The sound isolation performance of the optimized MPAF was compared to that of the full-band processor of 2048 taps per channel in Figure 6. The acoustic contrast simulation was done by filtering a unit impulse signal with the measured IRs and subband filter of Figure 5. The unit impulse signal was low-pass filtered by an extra filter to prevent excessive high frequency components near headrest loudspeakers. It can be seen that acoustic contrast similar to the full-band processing can be obtained with highly reduced number of filter taps. Especially, in high frequencies over 12 kHz, the acoustic contrast is unharmed even with the 128 taps MPAF filter. This is because the reverberation is not long in the high frequency region, and direct waves from headrest loudspeakers near the bright zone contribute dominantly to the high frequency response. Therefore, a long filter is not required to control interferences between distant loudspeakers.

The computational cost of the subband structure is much lower than the cost of the full-band processing. Since the computational costs of the upsampling, downsampling, and integer time delay are negligible, only the analysis and synthesis filters and MPAFs are mainly responsible for the total load of the system. In the proposed design, a total of 25×10 (analysis) + 25×10×18 (synthesis) + 800×18 (MPAF) = 19150 taps of FIR coefficients were used, which is approximately 52% of the number of filter taps required for the full-band processing (2048×18=36864 taps).

Finally, to check the equalization and time alignment between subbands, the impulse and frequency responses at the reference position were inspected (Figure 7). The result shows the frequency response almost similar to that of the full-band processing without noticeable discontinuity at the edges of the individual subbands. The impulse response of the proposed structure is also aligned in time domain well but exhibits more time delay due to delays of the multistage QMF filters. However, the total amount of latency (44 ms) induced by this time delay is not significant for most of audio playback applications.

4. SUMMARY

A subband optimization and filtering technique was introduced to reduce the computational effort of personal audio systems. The proposed technique utilizes the QMF structure to selectively optimize MPAFs for individual subbands. In this paper, it is described how subband filters should be equalized and aligned to produce output signals with negligible distortion. The simulation conducted using IRs measured in a real car cabin shows that by using the QMF subband structure, the number of filter taps can be reduced for each individual subband. Finally, the total number of FIR filter taps can be reduced by 50% compared to the original full-band design without sacrificing the acoustic contrast.

Table 1. Subband specifications

Subband No.	**1**	**2**	**3**	**4**	**5**	**6**
Frequency (kHz)	0–0.75	0.75–1.5	1.5–3	3–6	6–12	12–24
IR length (samples)	300	300	600	1200	2400	4800
MPAF taps	64	80	128	200	200	128

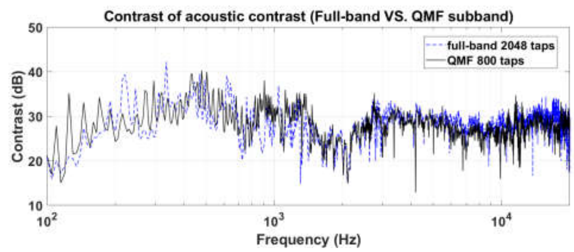

Figure 6. Comparison of simulated acoustic contrast for the full band (dashed line) and subband (solid line) processing using QMF structure.

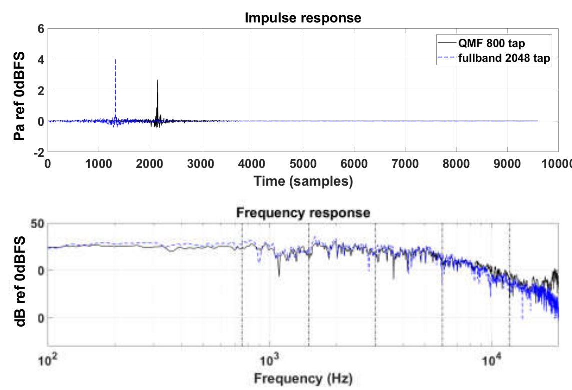

Figure 7. Final impulse response (top) and frequency response (bottom) after the subband filtering, measured at the reference microphone (microphone near the center of the bright zone). Vertical dashed line: subband cutoff frequencies.

ACKNOWLEDGEMENT

This research was financially supported by the Korea evaluation institute of industrial technology (KEIT, Korea) and the Ministry of Trade, Industry & Energy (MOTIE, Korea) through the core technology development program of the Automotive Industry (10082561, Development of Sound Field Control System for Realizing Personal Sound Zone in Vehicle Interior).

REFERENCES

[1] W. F. Druyvesteyn and J. Garas, "Personal Sound," *J. Audio. Eng. Soc.*, 45(9), pp. 685–701, Sep. 1997.

[2] C. H. Lee, J. –H. Chang, J. Y. Park, and Y. –H. Kim, "Personal sound system design for mobile phone, monitor, and television set; Feasibility study," *J. Acoust. Soc. Am.*, 122(5), p. 3053, 2007.

[3] J. -Y. Park, J. –H. Chang, Y. –H. Kim, "Generation of Independent Bright Zones for a Two-Channel Private Audio System," *J. Audio. Eng. Soc.*, 58(5), pp.382–393, Jun. 2010.

[4] S. J. Elliott, J. Cheer, J. –W. Choi, Y. Kim, "Robustness and regularization of personal audio systems," *IEEE Trans. Audio Speech Lang. Process.*, 20(7), pp.2123–2133, Sep. 2012.

[5] J. Cheer, S. J. Elliott, and M. F. S. Gálvez, "Design and implementation of a car cabin personal audio system," *J. Audio Eng. Soc.*, 61(6), pp. 414–424, 2013.

[6] J. –W. Choi, Y. –H. Kim, "Generation of an acoustically bright zone with an illuminated region using multiple sources," *J. Acoust. Soc. Am.*, 111(4), pp.1695–1700, Apr. 2002.

[7] J. –W. Choi, Y. –H. Kim, "Active Control for the Enhancement of Sound Field," *in Proc. of Active 04*, Williamsburg, Virginia, 2004.

[8] J. -W. Choi, "Sound shaping: Shaping sound in space and time using loudspeaker arrays," *in Proc. of Inter-Noise 2014*, Plenary Lecture, Melbourne, Australia, November 16-19, 2014.

[9] J. –W. Choi, "Subband optimization for acoustic contrast control," *in Proc. of International Congress on Sound and Vibration 22*, Florence, Italy, July 2015.

[10] Y. Cai, M. Wu, L. Liu, J. Yang, "Time-domain acoustic contrast control design with response differential constraint in personal audio systems," *J. Acoust. Soc. Am.*, 135(6), EL252-EL257, 2014.

[11] M. F. S. Gálvez, S. J. Elliott, and J. Cheer, "Time Domain Optimization of Filters Used in a Loudspeaker Array for Personal Audio," *IEEE/ACM Trans. Audio Speech Lang. Process.*, 23(11), pp. 1869-1878, 2015.

[12] M. Poletti, "An investigation of 2-d multizone surround sound systems", *in Proc. of the 125th Audio Eng. Soc. Conv.*, San Francisco, CA, 2-5 October 2008.

[13] Y. Wu and T. D. Abhayapala, "Spatial multizone soundfield reproduction: Theory and design," *IEEE Trans. Audio Speech Lang. Process.*, 19(6), pp. 1711–1720, 2011.

[14] M. A. Poletti and F. M. Fazi, An approach to generating two zones of silence with application to personal sound systems. *J. Acoust. Soc. Am.*, 137(2), pp. 598-605, 2015.

[15] W. Zhang, T. D. Abhayapala, T. Betlehem, F. M. Fazi, "Analysis and control of multi-zone sound field reproduction using modal-domain approach," *J. Acoust. Soc. Am.*, 140(3), pp. 2134-2144, 2016.

[16] T. Betlehem and P. D. Teal, "A constrained optimization approach for multizone surround sound," *in Proc. IEEE Int. Conf. Acoustics, Speech, Signal Process.*, Prague, Czech Republic, pp. 437–440, May 2011.

[17] J. –H. Chang and F. Jacobsen, "Sound field control with a circular double-layer array of loudspeaker," *J. Acoust. Soc. Am.*, 131(6), pp. 4518–4525, 2012.

[18] P. Coleman, P. Jackson, M. Olik, and J. A. Pederson, "Optimizing the planarity of sound zones," *in Proc. 52nd Int. Conf. of Audio Eng. Soc.*, Guildford, U.K., Sept. 2013, pp. 1–10.

[19] Y. Cai, M. Wu, J. Yang, "Sound reproduction in personal audio systems using the least-squares approach with acoustic contrast control constraint," *J. Acoust. Soc. Am.*, 135(2), pp. 734–741, Feb. 2014.

[20] P. Coleman, P. J. Jackson, M. Olik, M. Møller, M. Olsen and J. A. Pedersen, "Acoustic contrast, planarity and robustness of sound zone methods using a circular loudspeaker array," *J. Acoust. Soc. Am.*, 135(4), pp.1929-1940, 2014.

[21] S. Goose, L. Riddle, C. Fuller, T. Gupta and A. Marcus, "PAZ: In-Vehicle Personalized Audio Zones," *IEEE Multimedia*, 23(4), pp. 32-41, Oct.-Dec. 2016.

[22] A. Croisier, D. Esteban, and C. Galand, "Perfect channel splitting by use of interpolation/decimation/tree decomposition techniques," *in Proc. of the International Symposium on Information Circuits and Systems*, Patras, Greece, 1976.

[23] J. D. Johnston, "A Filter Family Designed for Use in Quadrature Mirror Filterbanks," *in Proc. of IEEE International Conference on Acoustics, Speech and Signal Processing*, Denver, 1980, pp. 291-294.

[24] T. Q. Nguyen and P. P. Vaidyanathan, "Two-channel perfect-reconstruction FIR QMF structures which yield linear-phase analysis and synthesis filters," *IEEE Trans. Acoust. Speech Sig. Processing*, 37(5), pp. 676–690, 1989.

[25] A. K. Soman, P. P. Vaidyanathan, and T. Q. Nguyen, "Linear phase paraunitary filter banks: theory, factorizations and designs," *IEEE Trans. Sig. Process.*, 41(12), pp. 3480–3496, 1993.

[26] S. -J. Yang, J. -H. Lee, and B. -C. Chieu, "Perfect-reconstruction filter banks having linear-phase FIR filters with equiripple response," *IEEE Trans. Sig. Process.*, 46(12), pp. 3246–3255, 1998.

[27] J. Soo and K. Pang, "Multidelay block frequency domain adaptive filters," *IEEE Trans. Acoust. Speech, Sig. Processing*, 38(2), 373–376, 1990.

[28] J. Borrallo and M. Otero, "On the implementation of a partitioned block frequency domain adaptive filter (PBFDAF) for long acoustic echo cancellation," *Signal Processing*, 27(3), 301-315, 1992.

[29] D. R. Morgan and J. C. Thi, "A delayless subband adaptive filter architecture", *IEEE Trans. Signal Processing*, 43(8), 1818-1830, 1995.

[30] S. J. Park, J. H. Yun and Y. C. Park, "A delayless subband active noise control system for wideband noise control", *IEEE Trans. Speech and Audio Processing*, 9(8), 892-899, 2001.